Available online at www.sciencedirect.com
ScienceDirect
Earth and Planetary Science Letters 258 (2007) 428–441
EPSL
www.elsevier.com/locate/epsl

Plate acceleration: The obduction trigger?

P. Agard [a,*], L. Jolivet [a], B. Vrielynck [a], E. Burov [a], P. Monié [b]

[a] Laboratoire de Tectonique, UMR CNRS 7072, Université Pierre et Marie Curie - Paris 6, Case 129, Tour 46-0, 2E, 4 pl. Jussieu, 75252 Paris Cedex 05, France

[b] Laboratoire Dynamique de la Lithosphère, UMR CNRS 5573, Université Montpellier 2, Place E. Bataillon, 34095, Montpellier Cedex 05, France

Received 24 March 2006; received in revised form 30 March 2007; accepted 2 April 2007
Available online 11 April 2007
Editor: C.P. Jaupart

Abstract

Obduction processes, though spectacular (dense oceanic ophiolites are emplaced on top of light, continental rocks along thousands of km), have been little elucidated since the advent of plate tectonics. Based on convergence velocities and blueschist formation, we show that the two recent large-scale, Upper Jurassic and Upper Cretaceous obductions coincided with periods during which velocities increased abruptly and more than doubled. The latter obduction also modified the interplate coupling across adjacent subduction zones. We critically propose a mechanism in which large-scale obductions are triggered by intraplate instabilities resulting from sharp plate accelerations, possibly in response to superplume events.

Keywords: obduction; plate velocities; subduction; blueschists; superplume

1. Introduction

Obduction corresponds to one of plate tectonics oddities, whereby dense, oceanic rocks (ophiolites) are thrust on top of light, continental ones [1,2]. The Peri-Arabic obduction [3] corresponded to a spectacular, almost synchronous thrust movement along thousands of km from Turkey to Oman (in c. 5–10 Ma, see below; Fig. 1a), and across several hundreds of km. Such large-scale thrusts of obducted ophiolites, which represent our only oceanic record before c. 170 Ma, have been reported from most convergent belts [4,5], yet obduction processes are still poorly understood ("ophiolite emplacement is a vast topic covered by an abundant literature and a profusion of models, often poorly supported by facts"; [6]). Debates hinged on exact geodynamic settings [7–9] and emplacement modes [7,8,10–13], ranging from local (e.g., back-arc closure or underplating during subduction [14–16]) to large-scale thrusts associated with intraoceanic subduction [3,17], rather than on mechanisms triggering obduction.

Although obduction processes only represent 1% of today's convergence settings, age compilations of large-scale obducted ophiolites reveal striking age clusters [6,18]. Abbatte et al. [18] proposed to relate obduction time clusters to the supercontinent Wilson cycles. Based on a new worldwide compilation, Vaughan and Scarrow [4] recently proposed that obduction might correspond to episodic pulses related to superplume events. The above mentioned Peri-Arabic obduction

* Corresponding author. Tel.: +33 1 44 27 52 35; fax: +33 1 44 27 50 85.
E-mail address: philippe.agard@lgs.jussieu.fr (P. Agard).

0012-821X/$ - see front matter © 2007 Published by Elsevier B.V.
doi:10.1016/j.epsl.2007.04.002

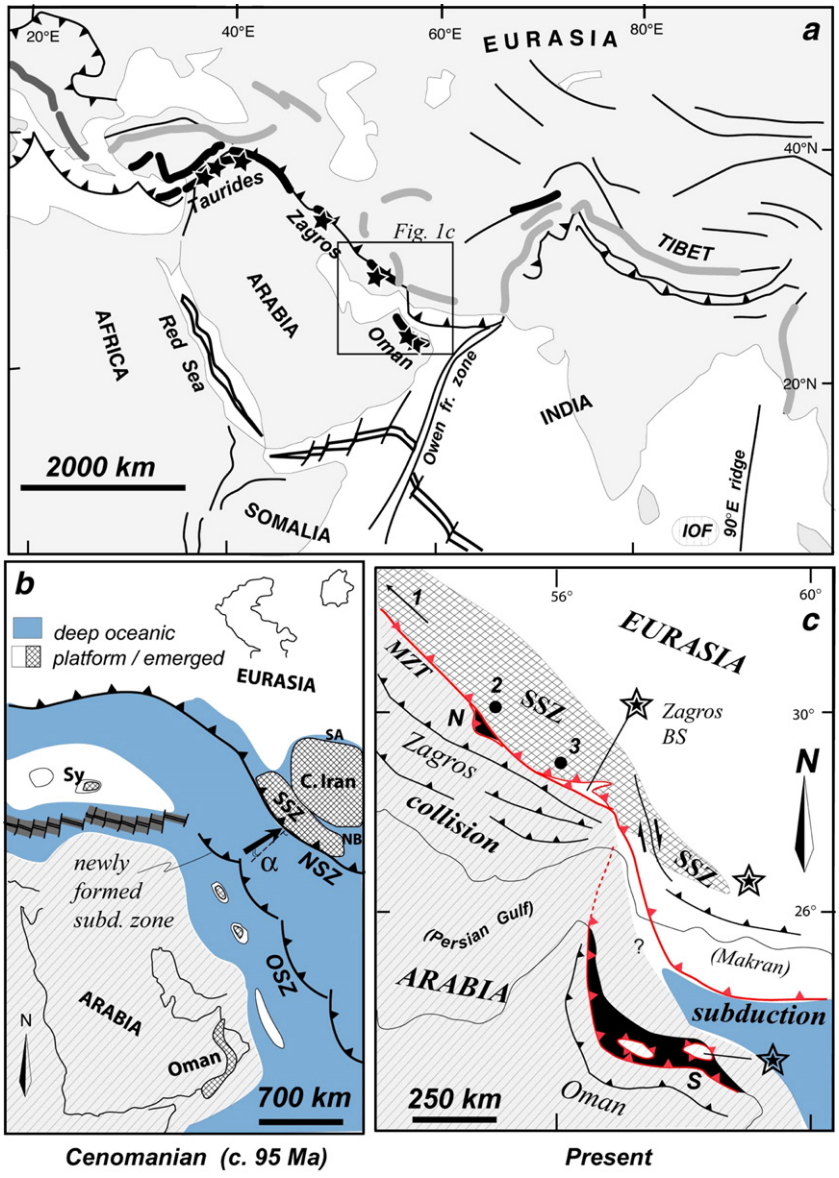

Fig. 1. a) Main ophiolite occurrences (thick lines) in the Alpine–Himalayan region. Ophiolites from the Upper Cretaceous Peri-Arabic obduction and from the Upper Jurassic Albania–Serbia obduction are shown in black and dark grey, respectively. Ocean folds in the Indian oceanic lithosphere are also indicated (IOF), as well as major faults and thrusts. Stars: localities where metamorphic soles underlying the Cretaceous ophiolite were dated (see Fig. 2a). b) Palaeogeographic map at c. 95 Ma [21,22] of the Neotethyan realm just after the intraoceanic subduction zone leading to ophiolite emplacement (OSZ) formed. C. Iran: Central Iran; NSZ: northern subduction zone below Eurasia; NB: Nain-Baft; SA: Sabzevar; SSZ: Sanandaj–Sirjan zone; Sy: Syria; α and arrow: convergence direction and obliquity, respectively, across the NSZ (see Fig. 2b and text). c) Present-day geodynamic configuration. N: Neyriz; S: Semail; SSZ: as above. 1, 2, 3: sites formerly lying on the NE edge of Arabia for which convergence velocities with respect to Eurasia were calculated (Fig. 2b). Stars: blueschist occurrences.

indeed followed the onset of the 120–80 Ma superplume [19] which caused major changes to the Earth system (e.g., emplacement of vast basalt plateaux, uniform geomagnetic superchron, high atmospheric CO2 concentration, etc.) and was possibly triggered by a mantle avalanche [20].

In order to further elucidate obduction mechanisms, we investigated convergence velocities and blueschists formation for the two major recent examples [4,6,18] for which regional-scale, geodynamic constraints are still accessible, namely for the large-scale Upper Jurassic and Upper Cretaceous obductions.

2. Triggering of the Semail obduction: a synchronous event along thousands of km

The Semail ophiolite has been the focus of numerous studies and is by far the best exposed of all obducted ophiolites (150 km × 600 km), having escaped Arabia/Eurasia collision (Fig. 1a), unlike other remnants of the Peri-Arabic obduction from Iran to Turkey (Fig. 1b,c; [3,21,22]). The geodynamic context of this Upper-Cretaceous obduction is somewhat puzzling, however (the Semail conundrum; [5,23]), as the geochemistry of upper ophiolite rocks, with arc signatures advocating for intraoceanic subduction, generally conflicts with tecto-nostratigraphic studies suggesting that the ophiolite formed near an active spreading ridge [7,24,25].

Three interpretations prevail at present in the literature. Based on the ophiolite's mantle flow structures, a number of workers have proposed that thrusting and subduction initiated at the locus of the Neotethyan ridge [6,24,25]. Others assume [9,13,26] that a genuine intraoceanic, NE-vergent subduction formed in the southern Neotethyan realm and allowed for a large oceanic obduction thrust to develop (Fig. 1b). This latter hypothesis accounts for the presence of calc–alkaline signatures as well as the possible formation of an oceanic ridge in a supra-subduction, back-arc context [27]. There is a growing recognition, however, that most obducted ophiolites worldwide, including the one from Oman, in fact correspond to supra-subduction zone forearc and infant arc settings [9,28]. In any case, the high temperature metamorphic soles found below most obducted ophiolites [6,13] are thought to represent the relics of these initial, high temperature thrusts (at c. 700–800 °C and 10–20 km below the oceanic Moho; [29,30]) coeval with the initiation of a new subduction zone. In the case of the Neotethyan realm it should be noted that a NE-dipping, synthetic northern subduction zone (NSZ, Fig. 1b) already existed to the N of the oceanic domain at the time.

We first compiled available amphibole Ar/Ar and K/Ar age data for metamorphic soles from Turkey to Oman (Fig. 2; [7,8,29,31–34]). Ages reveal a striking synchronicity and cluster mainly between c. 97–92 Ma, generalizing the conclusions of Hacker and co-workers for Oman [7,29]. Since cooling ages of metamorphic soles testify to cooling in less than 5 Ma below amphibole closure temperatures (510 °C ± 25; [7,13,32]), obduction contractional stages associated with incipient oceanic subduction must have started at c. 100 Ma at the earliest. Fig. 2a shows that they were largely coeval along more than 3000 km. This giant obduction is also thought to have extended further E between India and Eurasia (Fig. 1a; [35,36]) but the lack of dated metamorphic soles, inconsistencies regarding the exact geodynamic setting (e.g., [37] and references therein) and the presence of ophiolites emplaced during the separation of the Indian and Seychelles blocks [38] prevent further evaluation. Sedimentary constraints in Oman (recalled in Fig. 2a) suggest that the obduction process was terminated by c. 75–70 Ma and that the ophiolite's motion relative to the margin was approx. 400 km at c. 2 cm/yr [8,39]. Numerous lithostratigraphic and radiometric constraints suggest that high-pressure low-temperature (HP-LT) metamorphism of the transiently subducted Arabian continental margin likely took place at c. 80 Ma [8,34]. Metamorphic age constraints are still debated, however [17,34,39–41], due to older ages that do not fit easily with this conceptual scheme (c. ≥ 110 Ma; e.g., [41,42]). These older ages were interpreted as reflecting the existence of an earlier subduction system involving a continental microblock, but conflicting geodynamic settings have been proposed so far [17,41].

3. Sharp increase of convergence velocities before the upper Cretaceous obduction

We then performed kinematic calculations in order to retrieve convergence velocities and clarify the regional geodynamic setting of the Upper Cretaceous obduction (Fig. 1b). The paleopositions of several points assumed to mark the NE edge of Arabia were calculated with respect to Eurasia during the period 135–70 Ma (Fig. 2b; see Appendix for details).

The following assumptions were made to evaluate the respective movement between Arabia and the SSZ (Fig. 1b): 1) the SSZ is attached to Eurasia during the period 135 to 70 Ma, 2) the NSZ strikes NW–SE (i.e., following the edge of the SSZ), 3) the northern edge of Arabia is now located some 50–70 km north of the MZT (points 1–3, Fig. 1c) due to collisional shortening [43], 4) kinematic paths for points 1–3 are calculated using the rotation pole data of Muller et al. [44] and the algorithms of Cox and Hart [45]. Assumption 1 is known to be somewhat erroneous due to the existence of two additional, short-lived oceanic seaways between Arabia and Eurasia (Nain-Baft, Sabzevar; Fig. 1b; [46,47]). The discrepancy between SSZ/Arabia and Eurasia/Arabia convergence velocities, however, should be very small since both domains opened during the Campanian and closed in the Paleocene (c. 83–60 Ma; [46–48]) and were characterized by discontinuous oceanic crust emplacement.

The results show that: 1) velocities increased sharply, more than doubled and reached 5–6 cm/yr during the

period 118–85 Ma; 2) velocities gradually decreased from 85 to 70 Ma and were stabilized at approx. 3–3.5 cm/yr towards the end of the Cretaceous, which compares with published estimates for the Early Tertiary (c. 3.2 cm /yr; [49]); 3) the convergence velocity decrease after 85 Ma was coeval with HP-LT metamorphism of the Arabian margin; 4) convergence directions changed markedly at 118 Ma and obliquity decreased. Comparison of Fig. 2a and b shows that obduction movements developed over a period during which the Neotethyan ocean shrunk twice as fast. Obduction followed c. 15 Ma after the abrupt increase of convergence velocities and the reorientation of convergence directions.

4. Further evidence: modification of interplate mechanical coupling in the adjacent Zagros subduction zone

We then investigated how obduction movements implying the formation of a new NE-vergent subduction zone affected subduction processes along the preexisting NSZ (Fig. 1b). Blueschist facies rocks (BS) formed as a result of HP-LT metamorphism in subduction zones, at the plates interface, provide a good record of such processes [50,51]. Despite a long-lasting subduction history across the NSZ (c. 150–35 Ma), it was recently shown [52] that BS were only exhumed in the NSZ, from depths around 35 km, during the period 100–85 Ma (and to a lesser extent 120–80 Ma; Fig. 2c). The comparison of Fig. 2b,c demonstrates that this transient BS exhumation along the NSZ coincided with the period of high convergence velocities and that exhumation stopped afterwards. Since subduction thermal regimes primarily depend on velocity changes in the range 3–12 cm/yr [53], it may also be that blueschists (i.e., testifying to a cooler subduction regime) formed more efficiently during the period of high convergence velocities. This BS exhumation, in any case, testifies to a crucial modification of interplate mechanical coupling across the NSZ during a transient period coeval with high convergence velocities and obduction movements. It is also worth pointing out that the other, rare BS remnants thought to have formed across the NSZ or a lateral equivalent (Turkey, Makran, Pakistan Himalaya; [54]) span the same age range between 80–88 Ma [55–57].

5. Further evidence, 2: the Jurassic obduction coincided with high convergence velocities

In order to confirm the above results, we investigated the obduction context of the well-preserved ophiolite exposures found from Serbia to Greece along approx. 1000 km (Fig. 1a). These ophiolites were emplaced during the Upper Jurassic through a SE thrusting onto Apulia and obduction was terminated well before 125 Ma [58,59]. Again, we compiled available radiometric Ar/Ar and K/Ar age constraints on hornblende from the ophiolite metamorphic soles ([58,60] and references therein). Ages cluster around 175–160 Ma (Fig. 2d), with a somewhat larger scatter than in the Cretaceous case. As for the Cretaceous obduction, we estimated convergence rates between Africa and Eurasia for the period 175–120 Ma (Fig. 2d). It should be noted, however, that, with respect to the Cretaceous case, details of the paleogeography and of the microblocks inbetween are not so well constrained [21,22,61]. Fig. 2d shows that the inception of the Jurassic obduction, as testified by ages obtained for metamorphic soles, also developed during a period of high convergence velocities. Owing to the lack of kinematic constraints prior to 175 Ma, it is unfortunately impossible to know whether obduction followed a jump in convergence velocities and, in this event, after which time lapse the metamorphic soles formed.

6. Discussion

6.1. Did an increase of horizontal plate velocities trigger obduction?

Our results demonstrate that obduction coincided with periods of high velocities for the two recent large-scale obductions in Earth's history that affected the same Neotethyan ocean, presumably at different thermal states. Further testing on other large-scale obduction settings [18] is impossible, unfortunately, due to ill-constrained kinematic parameters (e.g., Paleozoic or Himalayan ophiolites) or to large displacements of obducted terranes along strike (e.g., E-Pacific ophiolites). The velocity contrast in both cases was similar, with obduction periods characterized by horizontal velocities on the order of 6 cm/yr, whereas 'normal' periods peaked at 2–3 cm/yr only (Fig. 2). The good precision on convergence velocities, typically on the order of a few mm/yr with recent refinements [44] (see Appendix and Fig. 2b), ensures that the inferred differences in the velocities during the obduction and the 'normal' periods of plate convergence are ≥ 3 cm/yr. Despite almost constant average worldwide expansion rates over the last 180 Ma at approx. 3 cm/yr [62], this abrupt Cretaceous velocity increase across the Neotethys correlates well with the sharp increase of spreading rates at c. 118 Ma in the Atlantic (a lesser one is observed in

the Pacific and the Indian ocean; [62]). With respect to the relatively steady-state plate tectonic regime, where plate torques are compensated and minimized [63], this sharp rise of velocities (Fig. 2b) represents a very sudden acceleration compared to the time of visco-elastic relaxation in the lithosphere. In the case of the Jurassic obduction the rise of velocities is not accessible but a large deceleration is also observed after the obduction

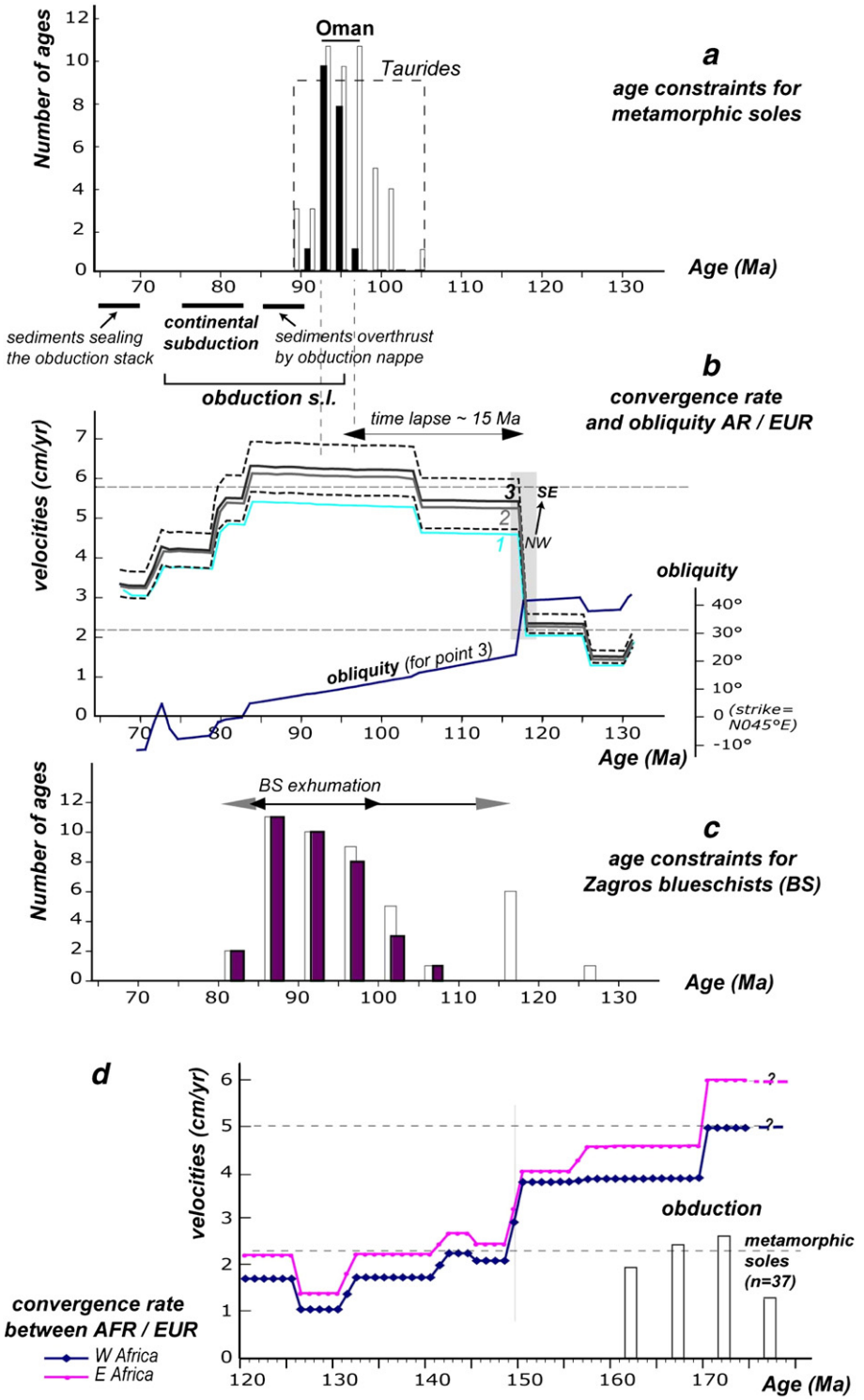

(Fig. 2d). Such a drastic change of tectonic boundary conditions must have had a large impact on the shrinking Neotethyan realm.

Most studies of subduction zones predict that velocity increase will modify interplate coupling [64–66] and enhance BS exhumation [67]. Analysis of subduction zone forces [64,68,69] generally outlines slab pull (resulting from negative buoyancy forces), slab anchor (i.e., forces resisting slab lateral migration with respect to trench), asthenosphere flow resisting slab edge progression, and friction (basal mantle drag, interplate coupling) as the main forces. The intraplate sections of most subducting plates being largely undeformed, it must be concluded that the net horizontal force acting within these plates should be small, significantly smaller then their yield limits.

Since viscous or visco-elastic rheology is the only one dependent on the velocity of deformation (strain rate), forces sensitive to convergence rate changes will likely be viscous forces acting at the lithosphere–asthenosphere interface and additional intraplate visco-elastic forces. Although thermally dependent forces (buoyancy, thermal stresses, and ductile shear) are sensitive to the advection rate, they cannot significantly change at a scale of just a few Myr due to the thermal inertia of the lithosphere [70]. Hence, neither slab pull, ridge push nor interplate brittle friction forces, which are not chiefly strain rate-dependent, can be significantly modified due to short-term variations of the convergence rate.

Given that the estimated values of slab-pull forces (10^{13} N/m;[71]) largely exceed those of the ridge push (10^{12} N/m), the force balance at the slab end will chiefly control the style of plate deformation (Fig. 3a). The resistance of the viscous asthenosphere to slab progression, F_{vf}, can be roughly estimated as being directly proportional to the slab velocity:

$$F_{vf} = 6\pi\mu_a R' \cdot V$$

where μ_a is the average viscosity of the slab–asthenosphere interface ($\sim 5\times10^{19}$ Pa s), R′ is a parameter related to the geometry of the slab and V is the trench normal kinematic velocity. The magnitude of the repulsion force F_{vf} is comparable to the slab-pull force, F_{sp} ($F_{sp}\sim F_{vf}$ [64]), whereas other forces acting on the slab end appear to be less important [65].

The sharp velocity increase from c. 2–3 to 6 cm/yr must therefore have resulted in the doubling of viscous resistance forces F_{vf} without affecting the other members of the force balance, thus resulting in a crucial force misbalance in the lower plate (Fig. 3a). In particular, both the horizontal and vertical components of the net force acting at the slab end could have changed sign; this force ($\sim 10^{13}$ N/m) had to become strongly compressive in the ridge direction, which obviously resulted in a marked modification of the NSZ subduction regime. The transient BS exhumation documented along the NSZ (Fig. 2c) could represent such a modification of interplate coupling in response to changing boundary conditions. A sharp increase of convergence velocity, possibly with the additional help of plate reorientation (Fig. 2b), therefore represents a possible mechanism for triggering strong compressional deformations such as compressional instability at the far end of the plate, ultimately leading to obduction.

6.2. What are the forces required for the initiation of obduction?

The widespread occurrence of ophiolite-related metamorphic soles ([6]; Table 12-I) and the fact that most obducted ophiolites correspond to infant arc settings ([28] and references therein) suggests that large-scale obduction processes require the creation of new intraoceanic subduction zones, whether induced or spontaneous [28,72]. As velocities sharply increased from c. 2–3 to 6 cm/yr and asthenospheric forces resisted slab progression along the NSZ at a time scale close to lithospheric Maxwell relaxation times (0.1 to 3–5 Myr), it is likely that the elastic stress built up and propagated in the oceanic lithosphere, resulting in compressional instability (buckling, folding). In the case of the Cretaceous obduction, a new, induced synthetic subduction zone effectively formed in the Neotethyan realm along a major weakness zone (the OSZ; Fig. 1b), either at the Neotethyan ridge ([6,11,24]; the internal resistance of the lithosphere

Fig. 2. a) Peri-Arabic metamorphic soles age constraints from the literature (from Turkey to Oman) advocate for a highly synchronous obduction thrust movement along thousands of km. Data compiled from [7,29,31,32]. b) Convergence velocities between Arabia and Eurasia during the period 135–70 Ma (for sites 1–3 located on Fig. 1c), estimated every Ma based on recent rotation pole data [44] (precision ~ a few mm/yr; see Appendix). Obliquity is taken as the angle between the normal to the NSZ and the convergence direction ($\alpha>0$ on Fig. 1b). Obduction developed approx. 15 Ma after the sharp rise of convergence velocities. c) Radiometric constraints [52] for Zagros blueschists (BS) formed in the NSZ (Fig. 1c), evidencing a transient exhumation during the period 100–85 Ma. d) Convergence velocities between Africa and Eurasia during the period 175–120 Ma versus age data for metamorphic soles (histogram to the lower right). The Eurasian reference point was chosen in stable Eurasia N of the Thornquist line in order to avoid loosely accreted Hercynian terranes [61].

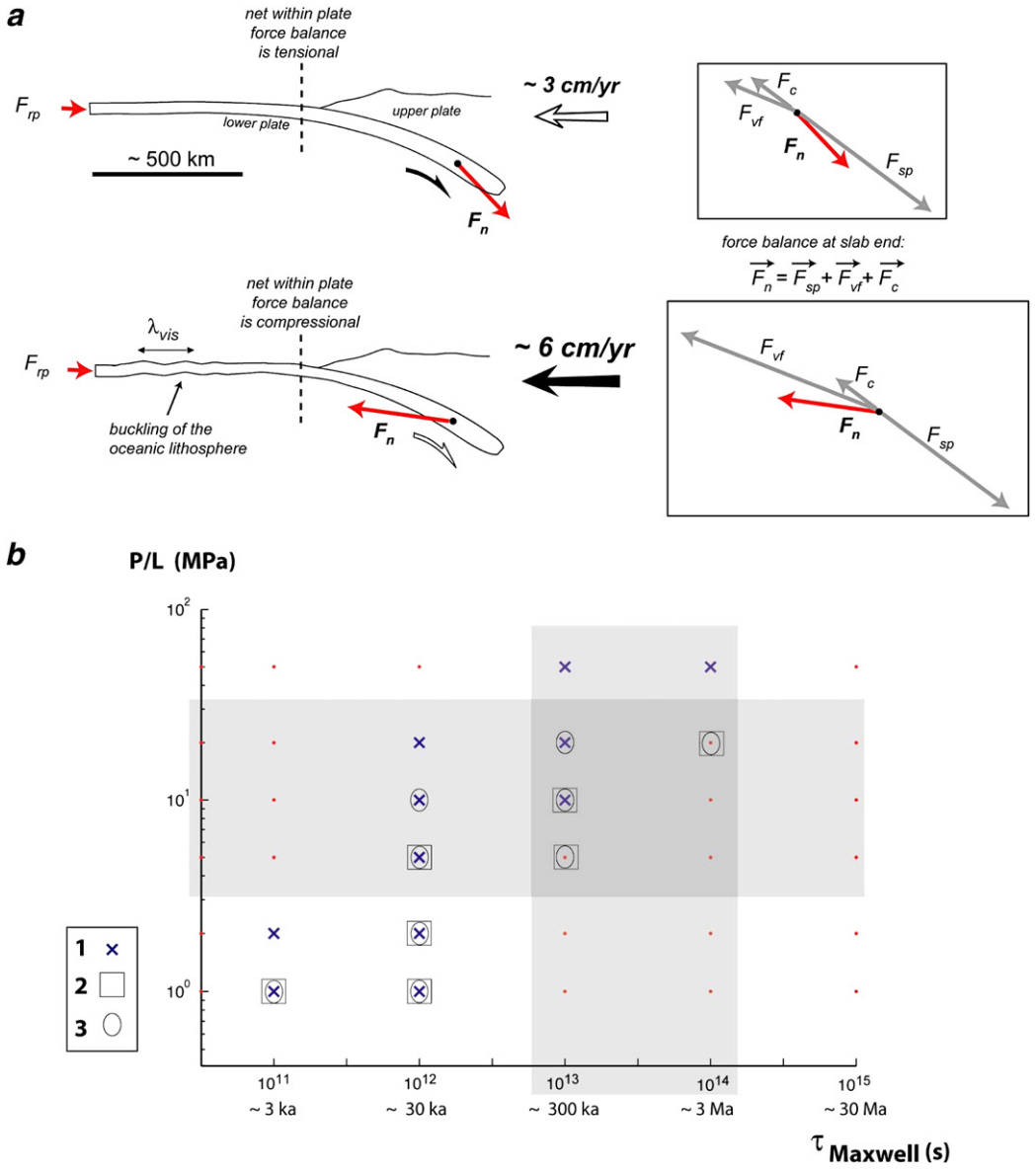

Fig. 3. a) Sketches depicting how the force balance within the lithospheric oceanic plate will be affected by the sharp rise of convergence velocities (Fig. 2b). The more than doubling of F_{vf} will result in a net force F_n reacting on the slab, which will possibly overwhelm F_{rp}. F_c: forces acting at the contact between the upper and lower plate; F_{rp}: ridge push force; F_{sp}: slab-pull force; F_{vf}: resistance asthenospheric force. See text for details. b) Plots of estimates of the maximal vertical deflection rate of buckling w_{max} falling in the range between 10^{-12} and 5.10^{-11} m/s for three different sets of parameters (1, 2 and 3 respectively correspond to he=50 km/L=500 km/Δh=100 m, he=40 km/L=500 km/Δh=10 m and he=70 km/L=1000 km/Δh=100 m). Values outside this range of strain rates are indicated by small dots. A value of 100 GPa was considered for Young's modulus [70]. It must be recalled that no universal analytical solution for visco-elastic folding in the presence of both gravity and rheology contrasts exists, and that only end-member analytical solutions or pure numerical solutions are available [82]. See text for further details.

is known to steadily increase away from the ridge [70]), or at a newly created fracture zone closer to the Arabian margin [8,13].

Present-day examples of strained oceanic lithosphere can be found in the central Indian Ocean folds (IOF, Fig. 1a; [73,74]) and the Zenisu ridge [75]. Gerbault [76], through modelling of the c. 200 km wavelength IOF, showed that the time lapse for the building up of intraplate forces was around 1–5 Ma and suggested that folding may ultimately lead to strain localization and subduction after another 10 Ma, as in analogue experiments [77] or envisioned by Stern [28].

Physical modelling of the initiation of subduction was attempted by several workers [69,78]. Experiments 4 and 5 of Shemenda [78] suggest that obduction (i.e., oceanic on top of continental) could develop, after a period of buckling and folding, whenever fractures or a sediment load are placed in the ocean–continent transition zone. Such pre-existing fractures (i.e., normal faults inherited from Permo-Triassic rifting) are notorious in the Peri-Arabic case.

In order to further constrain the mechanisms triggering obduction and evaluate forces required for obduction to proceed, we performed a simple parametric study of viscoelastic buckling or folding of the oceanic lithosphere. Note that in our view, buckling may not be a prerequisite to initiate an obduction thrust but rather provides an upper bound on the magnitude of the forces required. In the absence of gravity (density) contrasts, the maximal vertical deflection rate of buckling is given as [79]:

$$w_{\max} = \Delta h P Pe/(Pe - P)^2 \tau_m$$

where P is the net force characterizing the onset of folding in the oceanic lithosphere, Δh represents the amplitude of the initial vertical perturbation, τ_m is Maxwell relaxation time (i.e., the ratio of average plate viscosity μ over Young's modulus E) and the Euler load, Pe, which is the critical fiber force per unit length [80], is

$$\mathrm{Pe} = \pi^2 E h^3/(L^2 12(1-\nu^2))$$

(E=80–120 GPa and ν=0.25 are the elastic moduli; L=500–1500 km is plate length; h, the age-temperature dependent effective thickness of the oceanic lithosphere competent core, is around 35–50 km; [81]). It is noteworthy that ductile rheology laws for mantle olivine imply that plate viscosity μ is strongly depth dependent and may vary from 10^{19} at the base to 10^{26} Pa s at the top of the lithosphere (e.g., [76]).

The above equation for $w_{\max}$ yields the maximal folding rate developing in the absence of gravity forces for an infinite viscosity ratio between the folding layer and the substratum. There is no generalized analytical solution for visco-elastic folding, but end-member solutions show that if gravity forces due to density contrasts and finite competence contrasts were taken into account, the required folding force would differ and the dominant wavelength of folding would be smaller than for elastic buckling, yet still comparable [82]. Pure viscous folding, which may occur at any compressive horizontal force, provided sufficient competence contrast, is characterized by a wavelength λ_{vis} that depends on h and may be smaller than $L/2$ (Fig. 3a):

$$\lambda_{vis} = 2\pi h(\mu/6\mu_a)^{-1/3}$$

The fact that oceanic lithospheric folding is not such a widespread phenomenon implies that either (1) folding is a transient unstable mode of deformation, seldom preserved, that occurs during the initial stages of compression [≤10 My, e.g., 76], (2) the lithosphere exhibits finite elastic or plastic strength that requires a critical force threshold to be reached before the onset of folding, or (3) the lithosphere is found under very low internal strain rate (i.e., $<10^{-16}$ s^{-1}), as is the case of near steady-state subductions satisfying the following condition:

$$F_n \geq F_{rp} \geq 0$$

where F_n is the net force balance at the slab end and F_{rp} is the ridge push force (forces oriented trenchward are positive; Fig. 3a).

The results of our quantitative analysis, shown in Fig. 3b, indicate that realistic values of $w_{\max}$ (i.e., values between 10^{-12} and 5.10^{-11} m/s, based on available data for the IOF suggesting 1 km of vertical amplitude of folding within 1–10 Ma;[73,74,76]) are reproduced when applying stresses on the order of 10 MPa to the oceanic lithosphere over a time frame of 10^5 to several 10^6 y, and that the results are not greatly affected by variations in mechanical thickness. Although further numerical modelling of obduction is needed, these values, which are compatible with what is known from the magnitude of forces in the oceanic lithosphere [71], with recent estimates of the forces required for subduction initiation [72,83], and with the time constraints for the obduction recalled above, demonstrate in our view the feasibility of such a tectonic process.

6.3. A conceptual model for large-scale obductions (e.g., the Peri-Arabic obduction)

Based on the above results and discussion, a conceptual model for large-scale obductions is proposed (Fig. 4), in which the increase of convergence velocities results in an increased viscous repulsion of the subducting slab by the asthenosphere, and modifies the state of intraplate deformation and interplate coupling and BS exhumation in the NSZ (Fig. 4b).

As the velocity changes on a time scale (c. 1–2 My; Fig. 2b) comparable to that of visco-elastic relaxation in the lithosphere (0.1 – 3 My; Fig. 3b), slab repulsion

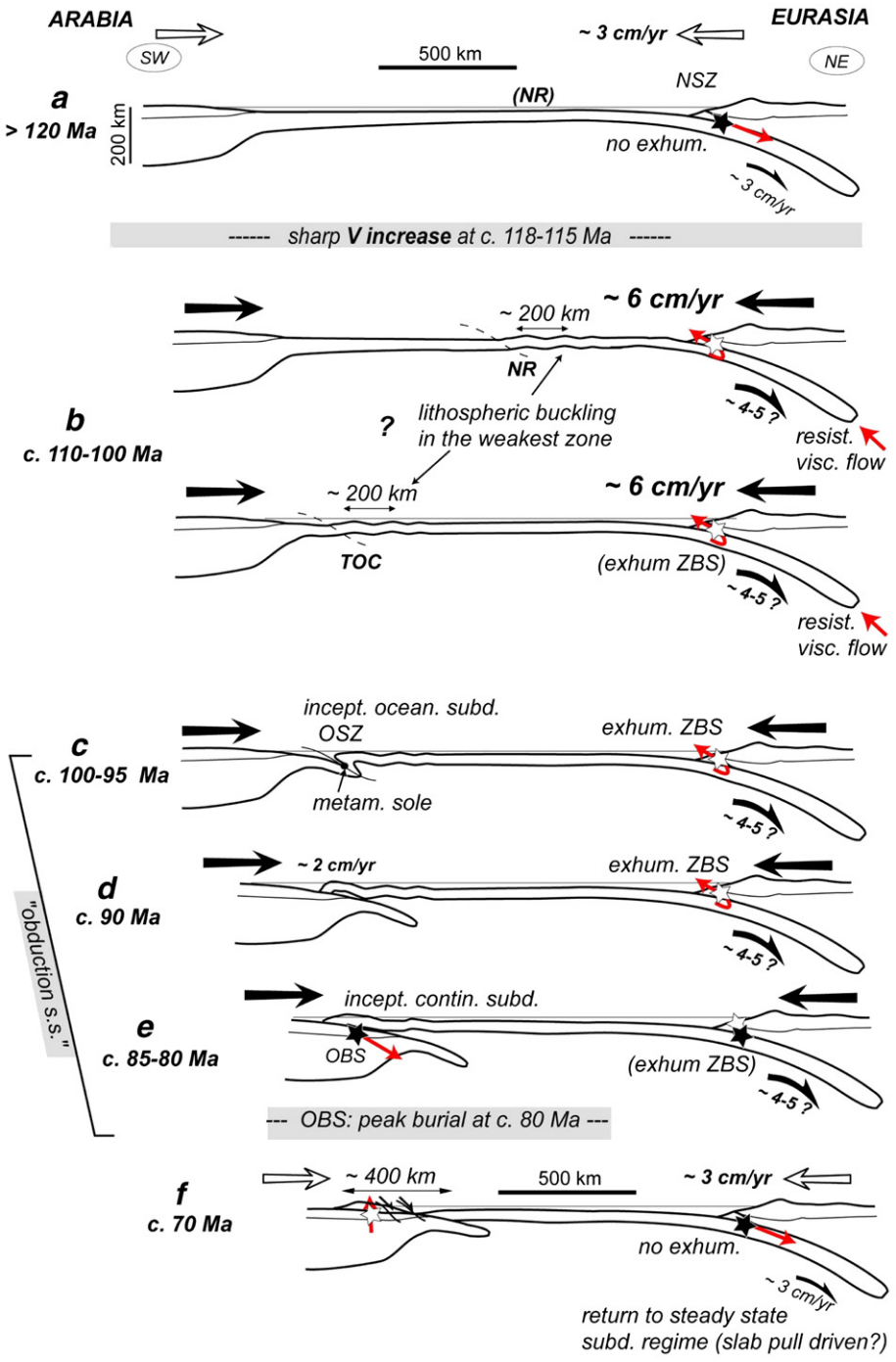

Fig. 4. Model mechanism for large-scale obduction trigger in response to an increase of convergence velocities. Increased resistance of the asthenospheric viscous flow in the existing subduction zone (NSZ; B; see also Fig. 3a) modifies the state of interplate coupling in the NSZ and BS exhumation ensues (b). Stresses accumulate in the oceanic lithosphere leading to buckling, rupture, and to the formation of a new subduction zone (OSZ; c). See text for details. NR: Neotethyan ridge; OBS and ZBS: Oman and Zagros blueschists; TOC: transition between ocean and continent.

should result in a visco-elastic reaction within the lower plate. For a stress relaxation time as high as 3 My in the competent core of the lithosphere, this reaction will affect the plate behaviour on the scale of at least 10 My [70]. Most importantly, since the change (increase) in the repulsion force is linearly proportional to the change in

velocity, the repulsion force should more than double and could exceed slab-pull forces ([64]; Fig. 3a). Our estimates suggest that a relatively small net compression force per unit length of c. 5×10^{12}–10^{13} N/m (i.e., 10 MPa averaged over a 1000 km plate; Fig. 3b) would be sufficient for the visco-elastic folding of the oceanic lithosphere. Note that this is the same magnitude as the one inferred from recent thermomechanical models for subduction initiation [72].

Folding will naturally first occur in the area where the lithosphere is the weakest (e.g., at the ridge, at a ridge-transform junction [7,28] and/or at the vicinity of the ocean–continent transition; Fig. 4b). Whereas the folding wavelength is proportional to the layer thickness, the folding curvature is inversely proportional to it. Bending stresses, which are highest in the area of highest curvature, may locally exceed intraplate stress by a factor of as much as 10^3 (e.g., [76]), locally reaching 0.5–1 GPa levels, and thus ultimately result in plate failure and deformation localization in the zone of smallest folding wavelength (since strength limits in the lithosphere do not exceed ~1 GPa [76]).

The time lapse between the velocity increase and the initiation of subduction, around 10–15 Ma (Fig. 2), would correspond to the time necessary for stresses to build up and for the oceanic lithosphere to buckle and break up. Once NE-dipping subduction along the OSZ is initiated at around 100–95 Ma (Fig. 4c), large-scale thrusting of the oceanic lithosphere occurs (Fig. 4d). Continental subduction, as the Arabian margin reaches the trench at approx. 85–80 Ma (Fig. 4e), soon (c. 5–10 Ma) chokes subduction processes in the OSZ and BS and eclogites are rapidly exhumed. The end of obduction and the decrease of convergence velocities (Fig. 2b) mark the end of BS exhumation in the NSZ (Fig. 4f). Extension, which closely followed the end of obduction (Fig. 2a), may correspond to the resumption of slab-pull forces across the NSZ (Fig. 4f).

Plate accelerations such as those reported here could result from major plate reorganizations and/or superplumes, the latter providing significant additional stresses (c. 10–100 MPa; [71]) over a relatively short time period (c. 1 Ma;[4]). In this line of thought, large-scale obductions would thus represent the lithospheric-scale consequence of deep mantle processes, in agreement with the emergent view that 'quiet' periods of plate tectonics are driven by long-term mantle convection, density contrasts and slab buoyancies [84], whereas pulses associated with superplumes and mixing of mantle reservoirs induce large-scale plate reorganizations [19,20,85]. Depending on the world-wide plate configuration and on the hotspot size [86], however, we anticipate that a superplume event will not necessarily be followed by a sharp enough jump of convergence velocities to trigger obduction in nearby oceans.

Acknowledgements

This research was supported by CNRS and the MEBE project.

Appendix A. Accuracy on kinematic velocity estimates

The finite rotation poles used for the velocity computation are those published by Muller et al. [44] for North America to Northwest Africa and for Eurasia to North America (Arabia remains fixed to Africa up to 30 Ma). In our work the reference point palaeopositions were calculated for each 1 Ma. Stage poles are computed for each step and velocity is deduced from the great circle arc length between the two relevant palaeopoints. To evaluate the possible discrepancy of these virtual point velocities, we computed the velocity between each point given by the published finite rotation poles. Poles available for both North America and Eurasia at a particular age are indicated by a dark grey overlay on Table 1 (only one pole is available otherwise; light grey is for North America, blank for Eurasia). Result columns in normal characters are those computed taking into account only the published poles, whereas those in italic were obtained with a step of 1 Ma. As a result the largest discrepancy on the speed calculation is 0.5 cm/year (delta column). Unfortunately, no published data allows computing the error due to the calculation of the published finite rotation poles.

It should be recalled that these pole ages are known with an uncertainty at worst equals to 2 Ma for the Northern Atlantic Ocean [44]. This ensures that the sharp increase of velocities documented at c. 118 Ma effectively took place within the grey bounds outlined in Fig. 2b. In order to evaluate the discrepancies associated with age uncertainties, the calculations were also performed with an average uncertainty of ±0.5 Ma on each time step (this is clearly an upper bound because it is equivalent to considering that the 65 My of the period 135–70 Ma may have lasted as much as 130 My or as little as 32 My): the results are shown as dotted lines for point 3. This shows that the magnitude of the discrepancy does not exceed c. 0.5 cm/year either.

For the sake of correlations, the chart of magnetic polarities, on which the work of Müller et al. [44] is based, is recalled facing Table 1.

Table 1
Evaluation of the discrepancies in estimating kinematic velocities

	Age	Paleo latitude	Paleo longitude	Angular distance	Kilometric distance	Speed	*Angular distance*	*Kilometric distance*	Speed	Delta
	69.0	23.32	44.56	0.8168	90.67	2.6	0.2738	30.43	3.0	−0.4
	72.5	22.64	44.07	0.6388	70.91	3.9	0.3026	33.62	3.4	0.5
	74.3	22.20	43.57	2.0151	223.68	3.8	0.3364	37.38	3.7	0.1
	80.2	20.62	42.23	1.7292	191.94	5.1	0.4175	46.39	4.6	0.5
	84.0	19.38	40.95	3.8747	430.09	5.4	0.4863	54.04	5.4	0.0
	92.0	16.96	37.77	6.2004	688.24	5.3	0.4800	53.34	5.3	0.0
	105.0	13.52	32.43	5.3858	597.82	4.6	0.4162	46.25	4.6	0.0
	118.0	11.16	27.48	1.4651	162.63	2.0	0.1828	20.31	2.0	0.0
	126.0	11.09	25.99	0.5741	63.72	1.2	0.1154	12.82	1.3	−0.1
	131.5	11.02	25.41	1.8763	208.27	2.2	0.1531	17.01	1.7	0.5

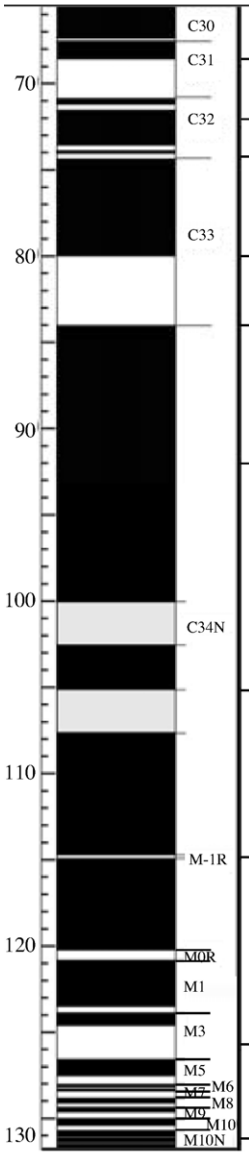

Result columns in normal characters are those computed taking into account only the published poles (column age), whereas those in italic were obtained with a step of 1 Ma. Poles available for both North America and Eurasia at a particular age are indicated by a dark grey overlay in the age column (only one pole is available otherwise; light grey is for North America, blank for Eurasia). The largest discrepancy on the speed calculation is 0.5 cm/yr (delta column). For the sake of correlations, the chart of magnetic polarities, on which the work of Müller et al. [44] is based, is recalled here. See Appendix for details.

References

[1] R.G. Coleman, Plate tectonic emplacement of upper mantle peridotites along continental edges, J. Geophys. Res. 76 (1971) 1212–1222.

[2] E.M. Moores, F.J. Vine, Troodos massif, Cyprus and other ophiolites as oceanic crust: evaluation and implications, Philos. Trans. R. Soc. Lond. 268A (1971) 443–466.

[3] L.E. Ricou, Le croissant ophiolitique péri-arabe, une ceinture de nappes mise en place au crétacé supérieur, Rev. Géogr. Phys. Géol. Dyn. 13 (1971) 327–350.

[4] A.P.M. Vaughan, J.H. Scarrow, Ophiolite obduction pulses as a proxy indicator of superplume events? Earth Planet. Sci. Lett. 213 (2003) 407–416.
[5] E.M. Moores, L.H. Kellogg, Y. Dilek, Tethyan ophiolites, mantle convection, and tectonic "historical contingency": a resolution of the "ophiolite conundrum", in: Y. Dilek, E.M. Moores, D. Elthon, A. Nicolas (Eds.), Ophiolites and oceanic crust: new insights from field studies and the ocean drilling program, Special Paper, vol. 349, Geological Society of America, Boulder, Colorado, 2000.
[6] A. Nicolas, Structures in Ophiolites and Dynamics of Oceanic Lithosphere, Kluwer, Dordrecht, 1989.
[7] B. Hacker, J.L. Mosenfelder, E. Gnos, Rapid emplacement of the Oman ophiolite: thermal and geochronologic constraints, Tectonics 15 (1996) 1230–1247.
[8] M.P. Searle, J. Cox, Tectonic setting, origin and obduction of the Oman ophiolite, Geol. Soc. Amer. Bull. 111 (1999) 104–122.
[9] J.W. Shervais, Birth, death, and resurrection: the life cycle of suprasubduction zone ophiolites, Geochem. Geophys. Geosyst. 2 (2001) (Paper 2000GC000080).
[10] R.G. Coleman, Tectonic setting for ophiolite obduction in Oman, J. Geophys. Res. 86 (1981) 2497–2508.
[11] A. Nicolas, X. Le Pichon, Thrusting of young lithosphere in subduction zones with special reference to structures in ophiolitic peridotites, Earth Planet. Sci. Lett. 46 (1980) 397–406.
[12] A. Michard, T. Juteau, H. Whitechurch, L'obduction : revue des modèles et confrontation au cas de l'Oman, Bull. Soc. Géol. Fr. 2 (1985) 189–198.
[13] J. Wakabayashi, Y. Dilek, What constitutes 'emplacement' of an ophiolite?: mechanisms and relationship to subduction initiation and formation of metamorphic soles, Ophiolites in Earth history Speciale Publication, vol. 218, Geological Society of London, London, 2003, pp. 427–447.
[14] C. Rangin, E.A. Silver, K. Tamaki, Closure of Western Pacific marginal basins: rupture of the oceanic crust and the emplacement of ophiolites, Active margins and marginal basins of the Western Pacific, Geophysical monograph, vol. 88, American Geophysical Union, 1995, pp. 405–417.
[15] C. Parkinson, Emplacement of the East Sulawesi ophiolite: evidence from subophiolite metamorphic rocks, J. Asian Earth Sci. 16 (1998) 13–28.
[16] M. Pubellier, C. Monnier, R. Maury, R. Tamayo, Plate kinematics, origin and tectonic emplacement of supra-subduction ophiolites in SE Asia, Tectonophysics 392 (2004) 9–36.
[17] J.P. Breton, F. Béchennec, J. Le Métour, L. Moen-Maurel, P. Razin, Eoalpine (Cretaceous) evolution of the Oman Tethyan continental margin: insights from a structural field study in Jabal Akhdar (Oman mountains), GeoArabia 9 (2004) 1–19.
[18] E. Abbatte, V. Bortolotti, P. Passerini, G. Principi, The rhythm of Phanerozoic ophiolites, Ofioliti 10 (1985) 109–138.
[19] R.L. Larson, Latest pulse of the Earth: evidence for a mid-Cretaceous superplume, Geology 19 (1991) 547–550.
[20] P. Machetel, E. Humler, High mantle temperature during Cretaceous avalanche, Earth Planet. Sci. Lett. 208 (2003) 125–133.
[21] J. Dercourt, L.E. Ricou, B. Vrielynck, Atlas Tethys Palaeoenvironmental maps, 14 maps, 1 pl., Gauthier-Villars, Paris, 1993.
[22] J. Dercourt, M. Gaetani, B. Vrielynck, E. Barrier, B. Biju-Duval, M.F. Brunet, J.P. Cadet, S. Crasquin, M. Sandulescu, Atlas Peri-Tethys, Palaeogeographical Maps: 24 Maps and Explanatory Notes, CCGM/CGMW, Paris, 2000.
[23] B. Hacker, E. Gnos, The conundrum of Semail: explaining the metamorphic history, Tectonophysics 279 (1997) 215–226.
[24] F. Boudier, G. Ceuleneer, A. Nicolas, Shear zones, thrusts and related magmatism in the Oman ophiolite: initiation of thrusting on an oceanic ridge, Tectonophysics 151 (1988) 275–296.
[25] A. Nicolas, F. Boudier, B. Ildefonse, E. Ball, Accretion of Oman and United Arab Emirates ophiolite — discussion of a new structural map, Mar. Geophys. Res. 21 (2000) 147–179.
[26] L. Beccaluva, M. Coltorti, G. Guiunta, F. Siena, Tethyan vs. Cordilleran ophiolites: a reappraisal of distinctive tectono-magmatic features of supra-subduction complexes in relation to the subduction mode, Tectonophysics 393 (2004) 163–174.
[27] S.J. Lippard, A.W. Shelton, I.G. Gass, The Ophiolite of Northern Oman, London, 1986 178 pp.
[28] R.J. Stern, Subduction initiation: spontaneous and induced, Earth Planet. Sci. Lett. 226 (2004) 275–292.
[29] B.R. Hacker, Rapid emplacement of young oceanic lithosphere: argon geochronology of the Oman ophiolite, Science 265 (1994) 1563–1565.
[30] R.A. Jamieson, *P–T* paths from high-temperature shear zones beneath ophiolites, J. Metamorph. Geol. 4 (1986) 3–22.
[31] R. Thuizat, H. Whitechurch, R. Montigny, T. Juteau, K–Ar dating of some infra-ophiolitic metamorphic soles from the Eastern Mediterranean: new evidence for oceanic thrustings before obduction, Earth Planet. Sci. Lett. 52 (1981) 302–310.
[32] O. Parlak, M. Delaloye, Precise 40Ar/39Ar ages from the metamorphic sole of the Mersin ophiolite (southern Turkey), Tectonophysics 301 (1999) 145–158.
[33] A.P. Onen, Neotethyan ophiolitic rocks of the Anatolides of NW Turkey and comparison with Tauride ophiolites, J. Geol. Soc. Lond. 160 (2003) 947–962.
[34] C.J. Warren, R.R. Parrish, D.J. Waters, M.P. Searles, Dating the geologic history of Oman's Semail ophiolite: insights from U–Pb geochronology, Contrib. Mineral. Petrol. 150 (2005) 403–422.
[35] A. Beck, D.W. Burbank, W.J. Sercombe, A.M. Khan, R.D. Lawrence, Late Cretaceous ophiolite obduction and Paleocene India–Asia collision in the westernmost Himalaya, Geodin. Acta 9 (1996) 114–144.
[36] M.P. Searle, R.I. Corfield, B. Stephenson, J. McCarron, Structure of the North Indian continental margin in the Ladakh–Zanskar Himalayas: implications for the timing of obduction of the Spontang ophiolite, India–Asia collision and deformation events in the Himalaya, Geol. Mag. 134 (1997) 297–316.
[37] J.C. Aitchison, Badengzhu, A.M. Davis, J. Liu, H. Luo, J.G. Malpas, R.C. McDermid, H. Wu, S.V. Ziabrev, M. Zhou, Remnants of a Cretaceous intra-oceanic subduction system within the Yarlung–Zangbo suture (southern Tibet), Earth Planet. Sci. Lett. 183 (2000) 231–244.
[38] E. Gnos, A. Immenhauser, T. Peters, Late Cretaceous/early Tertiary convergence between the Indian and Arabian plates recorded in ophiolites and related sediments, Tectonophysics 271 (1997) 1–19.
[39] M.P. Searle, C.J. Warren, D.J. Waters, R.R. Parrish, Structural evolution, metamorphism and restoration of the Arabian continental margin, Saih Hatat region, Oman Mountains, J. Struct. Geol. 26 (3) (2004) 451–473.
[40] C.J. Warren, R.R. Parrish, M.P. Searle, D.J. Waters, Dating the subduction of the Arabian continental margin beneath the Semail ophiolite, Oman, Geology 31 (10) (2003) 889–892.
[41] G.R. Gray, M. Hand, J. Mawby, R.A. Armstrong, J.M. Miller, R.T. Gregory, Sm–Nd and Zircon U–Pb ages from garnet-bearing eclogites, NE Oman: constraints on high-P metamorphism, Earth Planet. Sci. Lett. 222 (2004) 407–422.
[42] R. Montigny, O. Le Mer, R. Thuizat, H. Whitechurch, K–Ar and 40Ar–39Ar study of metamorphic rocks associated with the Oman

ophiolite: tectonic implications, Tectonophysics 151 (1988) 345–362.
[43] M. Molinaro, P. Leturmy, J.C. Guezou, D. Frizon de Lamotte, S.A. Eshraghi, The structure and kinematics of the southeastern Zagros fold-thrust belt, Iran: from thin-skinned to thick-skinned tectonics, Tectonics 24 (2005) doi:10.1029/2004TC001633.
[44] R.D. Müller, W.R. Roest, J.-Y. Royer, L.M. Gahagan, J.G. Sclater, Digital isochrons of the world's ocean floor, J. Geophys. Res. 102 (1997) 3211–3214.
[45] A. Cox, R.B. Hart, Plate Tectonics. How It Works, Blackwell, Oxford, 1986 392 pp.
[46] F. Baroz, J. Macaudière, R. Montigny, M. Noghreyan, M. Ohnenstetter, G. Rocci, Ophiolites and related formations in the central part of the Sabzevar range (Iran) and possible geotectonic reconstructions, Neues Jahrb. Geol. Paläontol. Abh. 168 (1984) 358–388.
[47] M. Arvin, P.T. Robinson, The petrogenesis and tectonic setting of lavas from the Baft ophiolitic melange, southwest of Kerman, Iran, Can. J. Earth Sci. 31 (1994) 824–834.
[48] A.M.C. Sengört. A new model for the late Palaeozoic–Mesozoic tectonic evolution of Iran and implications for Oman, in: A.H.F. Robertson, M.P. Searle, A.C. Ries (Eds.), The Geology and Tectonics of the Oman Region, Geological Society Special Publication, vol. 49, Geological Society of America, 1990, pp. 797–831.
[49] N. McQuarrie, J.M. Stock, C. Verdel, B.P. Wernicke, Cenozoic evolution of Neotethys and implications for the causes of plate motions, Geophys. Res. Lett. 30 (2003) doi:10.1029/2003GL017992.
[50] L. Jolivet, C. Faccenna, B. Goffé, E. Burov, P. Agard, Subduction tectonics and exhumation of HP metamorphic rocks of the Mediterranean orogens, Am. J. Sci. 303 (2003) 353–409.
[51] P. Agard, L. Labrousse, S. Elvevold, C. Lepvrier, Discovery of Palaeozoic Fe–Mg carpholite (Motalafjella, Svalbard Caledonides): a milestone for subduction zone gradients, Geology 33 (2005) 761–764.
[52] P. Agard, P. Monié, W. Gerber, J. Omrani, M. Molinaro, L. Labrousse, B. Vrielynck, B. Meyer, L. Jolivet, P. Yamato, Transient, syn-obduction exhumation of Zagros blueschists inferred from *P–T*, deformation, time and kinematic constraints: Implications for Neotethyan wedge dynamics, J. Geophys. Res. 111 (2006) B11401 doi:10.1029/2005JB004103.
[53] H. Staudigel, S.D. King, Ultrafast subduction: the key to slab recycling efficiency and mantle differentiation? Earth Planet. Sci. Lett. 109 (1992) 517–530.
[54] L.E. Ricou, Tethys reconstructed: plates, continental fragments and their boundaries since 260 Ma from Central America to South-eastern Asia, Geodin. Acta 7 (1994) 169–218.
[55] S.C. Sherlock, S.P. Kelley, S. Inger, N.B.W. Harris, A.I. Okay, 40Ar/39Ar and Rb–Sr geochronology of high-pressure metamorphism and exhumation history of the Tavsanli zone, NW Turkey, Contrib. Mineral. Petrol. 137 (1999) 46–58.
[56] M. Delaloye, J. Desmons, Ophiolites and melange terranes in Iran: a geochronological study and its paleotectonic implications, Tectonophysics 68 (1980) 83–111.
[57] R. Anczkiewicz, J.P. Burg, I.M. Villa, M. Meier, Late Cretaceous blueschist metamorphism in the Indus Suture Zone, Shangla region, Pakistan Himalaya, Tectonophysics 324 (1–2) (2000) 111–134.
[58] A. Dimo-Lahitte, P. Vergely, P. Monié, Metamorphic soles from the Albanian ophiolites: Petrology, 40Ar/39Ar geochronology, and geodynamic evolution, Tectonics 20 (2001) 78–96.
[59] A. Robertson, M. Shallo, Mesozoic–Tertiary tectonic evolution of Albania in its regional Eastern Mediterranean context, Tectonophysics 316 (2000) 197–254.
[60] J.G. Spray, J. Bébien, D.C. Rex, J.C. Roddick, Age constraints on the igneous and metamorphic evolution of the Hellenic–Dinaric ophiolites, Geological Society Special Publication 17 (1984) 619–627.
[61] G.M. Stampfli, G.D. Borel, A plate tectonic model for the Paleozoic and Mesozoic constrained by dynamic plate boundaries and restored synthetic oceanic isochrons, Earth Planet. Sci. Lett. 196 (2002) 17–33.
[62] J.P. Cogné, E. Humler, Temporal variations of oceanic spreading and crustal production rates during the last 180 My, Earth Planet. Sci. Lett. 227 (2004) 427–439.
[63] O. Cadek, Y. Ricard, Toroidal/poloidal energy partitioning and global lithospheric rotation during Cenozoic time, Earth Planet. Sci. Lett. 109 (1992) 621–632.
[64] C.H. Scholz, J. Campos, On the mechanism of seismic decoupling and back arc spreading at subduction zones, J. Geophys. Res. 100 (22) (1995) 22,103–22,115.
[65] A. Heuret, S. Lallemand, Plate motions, slab dynamics and back-arc deformation, Phys. Earth Planet. Inter. 149 (2005) 31–51.
[66] C.P. Conrad, S. Bilek, C. Lithgow-Bertelloni, Great earthquakes and slab-pull: interaction between seismic coupling and plate-slab coupling, Earth Planet. Sci. Lett. 218 (2004) 109–122.
[67] J.P. Platt, Calibrating the bulk rheology of active obliquely convergent thrust belts and forearc wedges from surface profiles and velocity distributions, Tectonics 19 (2000) 529–548.
[68] D. Forsyth, S. Uyeda, On the relative importance of the driving forces of plate motion, Geophys. J. R. Astron. Soc. 43 (1975) 163–200.
[69] C. Faccenna, D. Giardini, P. Davy, A. Argentieri, Initiation of subduction at Atlantic-type margins: insights from laboratory experiments, J. Geophys. Res. 104 (1999) 2749–2766.
[70] D.L. Turcotte, G. Schubert, Geodynamics, Cambridge University Press, Cambridge, 2002 456 pp.
[71] M.H.P. Bott, Modelling the plate-driving mechanism, J. Geol. Soc. Lond. 150 (1993) 941–951.
[72] M. Gurnis, C. Hall, L. Lavier, Evolving force balance during incipient subduction, Geochem. Geophys. Geosyst. 5 (2004) Q07001 doi:10.1029/2003GC000681.
[73] N. Chamot-Rooke, F. Jestin, B. de Voogd, P.w. group, Intraplate shortening in the Central Indian Ocean determined from a 2100-km-long north–south deep seismic reflection profile, Geology 21 (1993) 1043–1046.
[74] J.M. Bull, R.A. Scrutton, Fault reactivation in the Central Indian Ocean and the rheology of oceanic lithosphere, Nature 344 (1990) 855–858.
[75] S. Mazzotti, S.J. Lallemant, P. Henry, X. Le Pichon, H. Tokuyama, N. Takahashi, Intraplate shortening and underthrusting of a large basement ridge in the eastern Nankai subduction zone, Mar. Geol. 187 (2002) 63–88.
[76] M. Gerbault, At what stress level is the central Indian ocean lithosphere buckling? Earth Planet. Sci. Lett. 178 (2000) 165–181.
[77] J. Martinod, P. Davy, Periodic instabilities during compression of the lithosphere. 2. Analogue experiments, J. Geophys. Res. 99 (1994) 12,057–12,069.
[78] A.I. Shemenda, Horizontal lithosphere compression and subduction: constraints provided by physical modeling, J. Geophys. Res. 97 (1992) 11,097–11,116.
[79] A. Nadai, Theory of Flow and Fracture of Solids, McGraw-Hill, New York, 1963 705 pp.

[80] S. Timoshenko, J.N. Goodier, Theory of Elasticity, McGraw-Hill, N.Y., New York, 1970 567 pp.
[81] E.B. Burov, M. Diament, The effective elastic thickness (Te) of continental lithosphere: what does it really mean? J. Geophys. Res. 100 (1995) 3895–3904.
[82] S.M. Schmalholz, Y. Podladchikov, Viscoelastic folding: Maxwell versus Kelvin rheology, Geophys. Res. Lett. 28 (2001) 1835–1838.
[83] J. Toth, M. Gurnis, Dynamics of subduction initiation at preexisting fault zones, J. Geophys. Res. 103 (1998) 18,053–18,067.
[84] V. Deparis, H. Legros, Y. Ricard, Mass anomalies due to subducted slabs and simulations of plate motion since 200 My, Phys. Earth Planet. Inter. 89 (1995) 271–280.
[85] R.L. Larson, C. Kincaid, Onset of mid-Cretaceous volcanism by elevation of the 670 km thermal boundary layer, Geology 24 (1996) 551–554.
[86] V. Courtillot, A. Davaille, J. Besse, J. Stock, Three distinct types of hotspots in the Earth's mantle, Earth Planet. Sci. Lett. 205 (2003) 295–308.